Anal. Chem. **2005,** *77,* 4918−4926

A Dual-Frequency QCM-D Setup Operating at Elevated Oscillation Amplitudes

Malin Edvardsson,*,† Michael Rodahl,‡ Bengt Kasemo,† and Fredrik Höök*,†,§

Department of Applied Physics, Chalmers University of Technology, SE-412 96 Göteborg, Sweden, and Q-Sense AB, SE-426 77, Västra Frölunda, Sweden

An often raised, but rarely addressed, question with respect to applications of the quartz crystal microbalance technique is whether the shear oscillation of the sensor surface influences the adsorption kinetics or binding events being studied. Motivated by this uncertainty, as well as by the possibility of using elevated amplitudes to influence and steer specific biomolecular interactions, we have further developed the quartz crystal microbalance with dissipation monitoring (QCM-D) technique to operate in dual-frequency mode. One mode (one harmonic) is utilized for continuous excitation of the QCM-D sensor at resonance, at variable driving amplitudes, while the other mode (another harmonic) is used for combined frequency and energy dissipation (damping) measurements. To evaluate this experimental approach, we investigated the following: (i) the well-established process by which intact lipid vesicles adsorb and decompose into a planar supported lipid bilayer on SiO_2, recently shown to be very sensitive to external perturbations, and (ii) specific streptavidin binding to biotin-modified surfaces. In the former case, we observed a clear influence of elevated oscillation amplitudes on the bilayer formation kinetics, while in the latter case, no influence was observed for protein monomers. However, binding was inhibited when the biotin-binding protein was coupled to colloidal particles (o.d. ~200 nm).

The quartz crystal microbalance (QCM) is an ultrasensitive weighing device that utilizes the mechanical resonance of piezoelectric single-crystalline quartz.[1] This phenomenon, originally discovered by Pierre and Jacques Curie in 1880, is characterized by the ability of an external electric field to induce a mechanical strain in a material, where the direction of the induced strain can be controlled via the orientation of the cut with respect to the crystal lattice. When quartz crystals are utilized as weighing devices, so-called AT-cut crystals are usually used. The AT-cut ensures high-temperature stability and pure *shear* motion, when the sensor is subjected to an electric field. In the most common configuration, a thin (~200−400 μm) circular (o.d. ~0.5−3 cm) crystal disk is sandwiched between a pair of circular metal electrodes (usually gold), as schematically illustrated in Figure 1. By applying an ac voltage, resonance is excited when the frequency of the applied voltage corresponds to the resonance frequency, f_0, of the crystal. This resonance condition occurs when the thickness of the disk is an odd integer number of half-wavelengths of the standing wave induced between the electrodes, causing the mechanical oscillation to have its antinodes at each electrode surface:

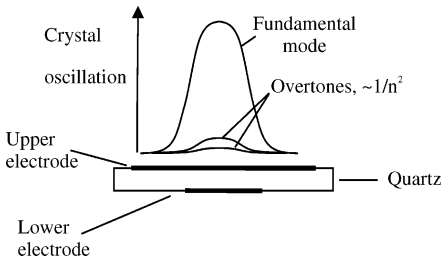

Figure 1. Schematic representation of a QCM crystal and the Gaussian amplitude distribution of the electrode immersed in aqueous solution. The overtone amplitudes are smaller than the fundamental mode one, and scales, as a first approximation, as $1/n^2$, where n (= 1, 3, ...) is the overtone number.

$$f_0 = nv_q/2t_q \quad (1)$$

where v_q is the wave velocity (speed of sound) in the quartz disk, t_q is the thickness of the disk, and n = 1, 3, ... is the overtone number. The resonant frequency of the crystal is thus proportional to the total mass (thickness × density) of the crystal. Provided that a mass added to one or both electrode surfaces is (i) small compared to the weight of the crystal, (ii) rigidly adsorbed, and (iii) evenly distributed over the active area of the crystal, eq 2 is applicable and tells that a change in the total mass of the crystal, Δm, induced upon adsorption is, to a first approximation, linearly proportional to a change in frequency, Δf:[2]

$$\Delta m = (C/n)\Delta f \quad (2)$$

where

$$C = t_q\rho_q/f_0 = -17.7 \text{ ng Hz}^{-1} \text{ cm}^{-2} \quad (3)$$

is the mass sensitivity constant for the crystal at 5 MHz.

* Corresponding authors. E-mail: maline@fy.chalmers.se; fredrik.hook@ftf.lth.se.

† Chalmers University of Technology.

‡ Q-Sense AB.

§ Current address: Division of Solid State Physics, Lund University, SE-221 00 Lund, Sweden.

(1) Salt, D. *Hy-Q Handbook of Quartz Crystal Devices*; Van Nostrand Reinhold: Wokingham, U.K. 1987.

10.1021/ac050116j CCC: $30.25
Published on Web 07/06/2005

Since the crystal oscillation is focused to the part of the crystal where the two circular electrodes overlap (see Figure 1), the amplitude of the mechanical motion (as well as the sensitivity to changes in mass) is highest at the center of the electrode area and diminishes in a Gaussian manner toward the edges of the electrodes (see Figure 1):[3]

$$A(r) = A_{\max} e^{-(r/c)^2} \quad (4)$$

where c is a Gaussian distribution coefficient determining the width of the sensitivity versus position curve and r is the distance from the center of the crystal.

Although the QCM technique was originally utilized for gas-phase and vacuum applications,[4] the work by Nomura and Hattori,[5] demonstrating that the QCM can also be used for liquid-phase applications, has paved the way for numerous applications, e.g., in biology, ranging from pure adsorption kinetics studies in the liquid phase to biosensor applications.[6−9] It was soon realized, however, that, in many of these studies, the adsorbed films do not obey the assumptions underlying eq 2. Generally this is connected with the fact that some or several of the conditions mentioned above for eq 2 to hold are not fulfilled. In particular, the combined effect of hydration water, water trapped between adsorbed species, and the nonrigid character of many polymers/biomolecules induces frictional (viscous) losses and thus a damping of the crystal's oscillation. This, in turn, violates the linear relation between Δf and Δm, and calls (i) for technical solutions that provide quantitative information not only about changes in resonance frequency but also about changes in energy dissipation, D, and (ii) for theoretical models that can analyze these data to obtain the desired information, e.g., adsorbed mass, even for these more complex cases.

Information about changes in D can indeed be obtained with sufficient resolution either via impedance spectroscopy[10] or, as done in previous work by our group, by recording the oscillation decay (the "ringing curve") of the crystal after rapid excitation at resonance.[11] By combining this type of multiparameter measurements with theoretical models including viscoelastic representations of nonrigid films,[12−14] detailed information about both the adsorbed mass and changes in the viscoelastic components of adsorbed films has been successfully obtained.[15]

In the present work, the information contained in combined f and D (QCM with dissipation monitoring, QCM-D) measurements has been further extended by simultaneously measuring f and D and using the *oscillation amplitude*, A, as an external control parameter/perturbation to influence the behavior of adsorbed macromolecules. Particular focus is placed on the often raised, but so far rarely addressed, question regarding the influence of the mechanical shear oscillation of the sensor surface, on the measured events. This is indeed a very relevant question. One general motivation is the often fragile character or multiplicity of relatively weak bonds that are responsible for the detailed architecture of biomacromolecules. Another more direct motivation derives from recent demonstrations of bond rupture in biological molecular complexes at elevated amplitudes in liquid-phase applications.[16,17] (The latter occurred although the amplitude of oscillation is orders of magnitude lower in the liquid than in the gas phase or vacuum, due to the high damping induced by the liquid (cf. eq 5).) In these studies, it was shown that hundreds of nanometer-to-micrometer-sized particles, which were bound to the sensor surface via multiple nonspecific interactions, specific protein−ligand interactions, or covalent bonds, could be detached from the oscillating sensor surface by increasing the force on the particles via increased oscillation amplitudes.[16−18]

In the present study, we have extended the exploration, and potential, of the QCM-D technique, by operating the device in dual-frequency mode, i.e., by using simultaneous excitation of the sensor at two different harmonics.[19] The two harmonics are used in two different modes, the "probe" and "actuator" modes, respectively: One harmonic is used as the probe for (decay-based) recording of changes in f and D, as in the original QCM-D device,[11] while the other harmonic is used as an actuator, for continuous excitation/perturbation with a variable driving amplitude (1−10 V). In contrast to previous work, this technical solution provides a means of using elevated amplitudes to perturb—or activate—binding reactions in a controlled way, while simultaneously maintaining the possibility to probe the adsorption or desorption events in a nonperturbative manner via combined f and D measurements, as the driving amplitude in the actuator mode is varied.

To evaluate the influence of the oscillation amplitude on biological binding reactions, three different model systems were investigated. These model systems were as follows: (i) the well-established process by which bilayer phospholipid vesicles in the liquid phase are adsorbed on a SiO_2 surface and eventually decompose and fuse into a planar supported phospholipid bilayer (SPB), a process known to be sensitive to external perturbations such as osmotic stress, temperature,[20] and mechanical stress exerted by an AFM tip, (ii) binding of the relatively rigid protein streptavidin (o.d. ∼6 nm; M_w ∼65 kDa) to a biotin-modified supported planar bilayer (biotin-SPB) of the same type as prepared in (i), and (iii) binding of polystyrene spheres (o.d. ∼200 nm; M_w

(2) Sauerbrey, G. *Z. Phys* **1959**, *155*, 206−222.
(3) Sauerbrey, G. *Archiv Elektr. Übertragung* **1964**, *18*.
(4) Alder, J. F.; MacCallum, J. J. *Analyst* **1983**, *108*, 1169−1189.
(5) Nomura, T.; Hattori, O. *Anal. Chim. Acta* **1980**, *115*, 323−326.
(6) Thompson, M.; Arthur, C. L.; Dhaliwal, G. K. *Anal. Chem.* **1986**, *58*, 1206−1209.
(7) Muratsugu, M.; Ohta, F.; Miya, Y.; Hosokawa, T.; Kurosawa, S.; Kamo, N.; Ikeda, H. *Anal. Chem.* **1993**, *65*, 2933−2937.
(8) Kösslinger, C.; Drost, S.; Aberl, F.; Wolf, H.; Koch, S.; Woias, P. *Biosens. Bioelectroni.* **1992**, *7*, 397−404.
(9) Kösslinger, C.; Drost, S.; Aberl, F.; Wolf, H. *Fresenius J. Anal. Chem.* **1994**, *349*, 349−354.
(10) Buttry, D. A.; Ward, M. D. *Chem. Rev.* **1992**, *92*, 1355−1379.
(11) Rodahl, M.; Kasemo, B. *Rev. Sci. Instrum.* **1996**, *67*, 3238−3241.
(12) Domack, A.; Prucker, O.; Rühe, J.; Johannsmann, D. *Phys. Rev. E* **1997**, *56*, 680−689.
(13) Philippoff, W. In *Physical Acoustics: Principles and Methods*; Mason, W. P., Thurston, R. N., Eds.; Academic Press: New York, 1988; Vol. 18.
(14) Voinova, M. V.; Rodahl, M.; Jonson, M.; Kasemo, B. *Phys. Scr.* **1999**, *59*, 391−396.
(15) Höök, F.; Kasemo, B.; Nylander, T.; Fant, C.; Sott, K.; Elwing, H. *Anal. Chem.* **2001**, *73*, 5796−5804.
(16) Cooper, M. A.; Dultsev, F. N.; Minson, T.; Ostanin, V. P.; Abell, C.; Klenerman, D. *Nat. Biotechnol.* **2001**, *19*, 833−837.
(17) Dultsev, F. N.; Ostanin, V. P.; Klenerman, D. *Langmuir* **2000**, *16*, 5036−5040.
(18) Dultsev, F. N.; Speight, R. E.; Florini, M. T.; Blackburn, J. M.; Abell, C.; Ostanin, V. P.; Klenerman, D. *Anal. Chem.* **2001**, *73*, 3935−3939.
(19) Vig, J. R. *1999 IEEE Ultrasonics symposium*.
(20) Reimhult, E.; Höök, F.; Kasemo, B. *Langmuir* **2003**, *19*, 1681−1691.

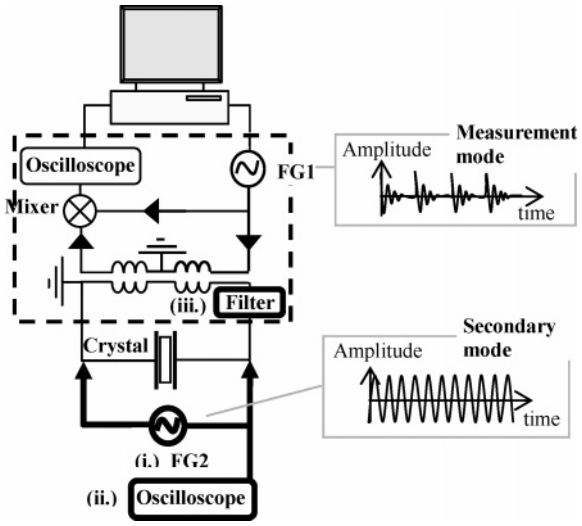

Figure 2. Schematic illustration of the modification made to the original setup (dotted square)[11] plus the components: (i) signal generator, (ii) oscilloscope, and (iii) filter, added to drive and probe the crystal in dual-frequency mode.

$\sim 2.67 \times 10^6$ kDa) modified with NeutrAvidin (a streptavidin analogue) to a biotin-SPB.

MATERIALS AN METHODS

Experimental Setup. To perform combined f and D measurements, while simultaneously varying the oscillation amplitude of the crystal in the actuator mode, an additional frequency generator was added to the original QCM-D setup.[11] One frequency generator (FG1, Agilent/HP) is used to excite crystal oscillation at one harmonic and the second frequency generator (FG2, HP) is operated in continuous mode at either a higher or a lower harmonic (Figure 2). To prevent FG2 from interfering with the measured decay signal, a suitable filter arrangement was used (Figure 2). Depending on whether the excitation frequency of FG1 was higher ($n_{FG1} > n_{FG2}$) or lower ($n_{FG1} < n_{FG2}$) than that of FG2, a low- (Mini Circuits BHP-25) or high-pass (Mini Circuits BLP-21.4) filter was used. The setup was used in two excitation modes: (mode I) decay-based (probe) measurements at 35 MHz, $n_{FG1} = 7$, with variable (actuator) driving amplitude (0−10 V) at 5 MHz, $n_{FG2} = 1$. (mode II) decay-based (probe) measurements at 15 MHz, $n_{FG1} = 3$, and variable (actuator) driving amplitude (0−10 V) at 35 MHz, $n_{FG2} = 7$.

Preparation of Lipids and Proteins. 1-Palmitoyl-2-oleoyl-*sn*-glycero-3-phosphocholine (850457P, Avanti Polar-Lipids) and 5% (w/w) 1,2-dipalmitoyl-*sn*-glycero-3-phosphoethanol amine-*N*-(Cap Biotinyl) (Biotin-PE, Avanti Polar-Lipids) were dissolved in chloroform and then evaporated with N_2 to form a thin lipid film on the wall of a glass flask. The film was hydrated with buffer (5 mg/mL; 10 mM Tris, 100 mM NaCl, pH 8) and extruded through polycarbonate membranes (Whatman) (15× through 0.1 μm and 15× through 0.03 μm) to form vesicles. The vesicle solution was stored at 4 °C under N_2 until use. Stock solutions of streptavidin (Sigma, 1 mg/mL in buffer) and biotin-albumin (Sigma, 1 mg/mL in Milli-Q grade water) were stored at −20 °C until use. A stock solution of NeutrAvidin labeled fluospheres (Molecular Probes) was stored at 4 °C until use, then mixed with buffer, and sonicated for 10 min immediately before use. The stock solution of PLL-PEG (biotin-derivatized poly(L-lysine)-*g*-poly(ethylene glycol), 10 mg/ml in 10 mM Hepes buffer, pH 7.4) was stored at −20 °C until use.

Surface Preparation. AT-cut quartz crystals coated with either Au or SiO_2 ($f_0 = 5$ MHz) were purchased from Q-Sense AB (Göteborg, Sweden). SiO_2-coated crystals were cleaned by immersion in 10 mM sodium dodecyl sulfate (SDS; >8 h) followed by twice rinsing with Milli-Q grade water, drying with N_2, and UV-ozone treatment (10 min). Gold-coated crystals were cleaned by boiling for 7 min in a solution of Milli-Q grade water, NH_3, and H_2O_2 (5:1:1). They were then rinsed with Milli-Q grade water and dried with N_2.

To eliminate parameter variation, measurements on SiO_2 were performed on one crystal per occasion, with in situ SDS (10 mM) cleaning between measurements, i.e., with the crystal remaining in the cell, followed by thorough rinsing in Milli-Q grade water. The reproducibility of the temporal variation (uptake kinetics) of f and D for bilayer formation on SiO_2-coated crystals was better than 2%. Measurements on gold-coated crystals were made on separate crystals, showing a reproducibility of better than 5%.

Relation between Driving Voltage and Oscillation Amplitude. The amplitude of oscillation of the quartz crystal has a Gaussian distribution across the electrode surface, with the maximum oscillation amplitude at its center. Not only is the oscillation amplitude dependent on the radial distance from the center, it is also dependent on overtone number ($n = 1, 3, ...$). The amplitude distribution through viscoelastic films probed in aqueous solutions was evaluated using the expressions presented by Kanazawa,[21] which also provide an estimate of the maximum (center) oscillation amplitude for a crystal oscillating with both sides in air or with one side immersed in water, with or without an adsorbed viscoelastic film. In the latter case, the film was represented by a uniform thickness, density, shear viscosity, and elastic modulus.[14] The obtained values of the amplitude at the center of the crystal (driving amplitude 1 V) in aqueous solution were 4.4 and 0.15 nm at 5 ($n = 1$) and 35 MHz ($n = 7$), respectively. However, experimental results reported by Borovsky et al.[22] have shown that, for AT-cut crystals, such as those used in the present study, the real maximum value is half the theoretical value; hence, $A_{mode\ I} \sim 2.2$ nm and $A_{mode\ II} \sim 0.07$ nm.

The amplitude of the crystal oscillation is expected to scale linearly (see below) with the voltage applied over the crystal, which is here referred to as the "load voltage". However, due to the high load impedance, the load voltage is not equivalent to the applied voltage. But since there is a linear dependence between the load voltage and the applied voltage, the maximum oscillation amplitude can still be precisely tuned—at least as long as the amplitude-induced change in frequency is small compared with the bandwidth of the resonance peak—see further below. Furthermore, since the load impedance depends on the oscillation frequency, it differs in mode I and mode II. The peak-to-peak load voltage (V_{pp}) was measured, with one side of the crystal immersed in an aqueous solution and found to be 16.4 V for mode I and 6.2 V for mode II, at a driving voltage of 10 V. Hence, the maximum crystal oscillation amplitudes, with one side immersed in water, were ~36.0 and 0.4 nm in mode I and mode II, respectively.

(21) Kanazawa, K. K. *J. Electroanal. Chem.* **2002**, *524−525*, 103−109.
(22) Borovsky, B.; Mason, B. L.; Krim, J. *J. Appl. Phys.* **2000**, *88*, 4017−4021.

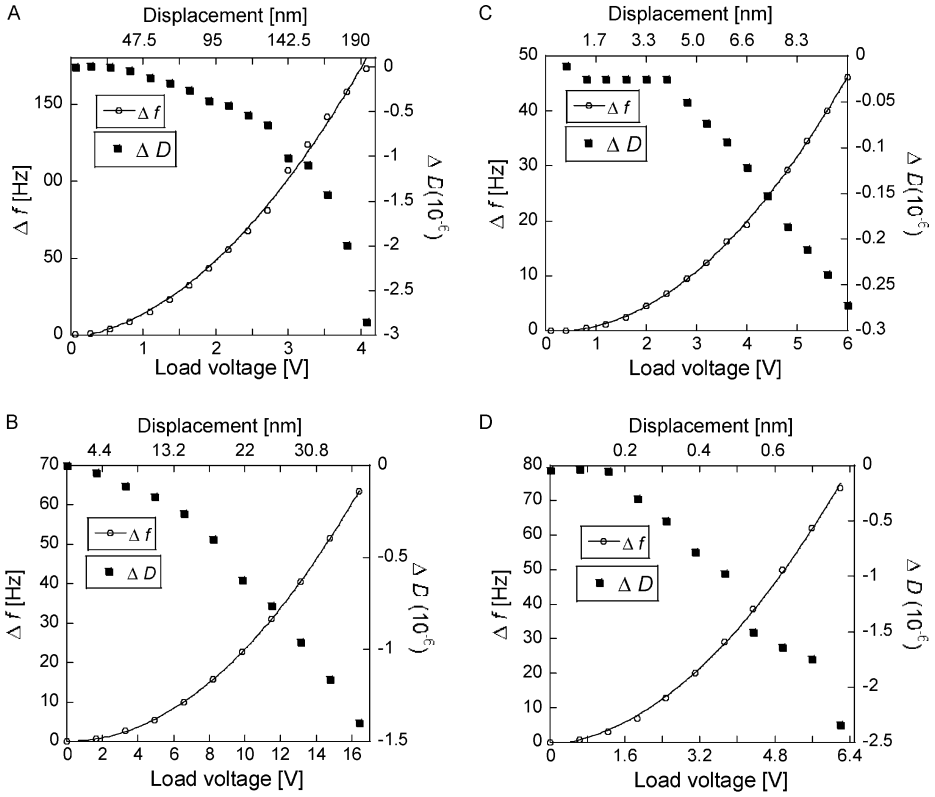

Figure 3. Changes in f (○) and D (■) versus load voltage (and oscillation amplitude) in air (A, C) and pure water (B, D) operated in mode I (A, B) and mode II (C, D). Also shown (—) is the fit to eq 6.

RESULTS AND DISCUSSION

Influence of Elevated Amplitudes on the Sensor Response. The influence of elevated amplitudes on changes in f and D when operating in the two (probe and actuator) modes was investigated for a bare crystal with one side exposed to air and the other exposed to either air or aqueous solution. Changes in f and D were recorded by decay-based measurements at 35 (mode I) or 15 MHz (mode II), as the nominal driving amplitude was varied between 0 and 10 V at 5 (mode I) or 35 MHz (mode II), respectively, for the measurements in aqueous solution and between 0 and 3 V in the air measurements. Qualitatively, the observed changes in f with varying driving amplitude (Figure 3) are in good agreement with the expected dependence on load voltage, U, and the motional resistance, R:[23]

$$\Delta f/f_0 = \alpha(U/R)^2 \qquad (5)$$

where α is a crystal-dependent constant that determines the stiffening of the quartz as the displacement increases. Note that the maximum change in frequency (~150 Hz) is orders of magnitudes lower than f_0. This means that stiffening has a negligible effect on the absolute amplitude of oscillation, and no deviation from a linear relation between applied voltage and crystal displacement is expected due to stiffening alone. However, since the frequency of the mode used to excite the crystal at elevated amplitudes was kept constant, the voltage-induced change in resonance frequency results in a mismatch between the excitation frequency and resonance peak position. Hence, if the bandwidth is small (Q is high), a deviation from a linear relation between the applied voltage and the oscillation amplitude is still expected. In the present case, the bandwidth, $\Delta f_{bw}(=Df_0)$, was ~100 Hz in air and 2 kHz in aqueous solution. Hence, in air, the observed changes in frequency are dominated by the voltage-induced change in the peak position of the resonance, while in aqueous solution, these effects can be neglected ($\Delta f_{loadvoltage}/\Delta f_{bw} < 0.04$). It should also be pointed out that, for a QCM crystal with one side immersed in an aqueous solution, the influence on f and D of an increase in temperature of the solution is also expected to scale with the square of the applied voltage (i.e., proportional to the input power). Furthermore, since the decrease in f and the increase in D induced by exposing one side of the crystal to an aqueous solution is proportional to $(\rho\eta)^{1/2}$, an increase in temperature of the solution will result in an increase in f and a decrease in D. The maximum decrease observed in D in aqueous solution (Figure 3) corresponds to ~1.5×10^{-6} (mode I) and ~2.5×10^{-6} (mode II). The bulk temperature was controlled via a Peltier element to 22 ± 0.1 °C, with a long-term temperature fluctuation of ±0.01 °C. This means that long-term temperature variations are efficiently controlled, and the observed changes in f and D upon increasing the drive amplitude can be evaluated based on the known temperature dependence of viscosity and density and the proportionality between changes in f and D and $(\rho\eta)^{1/2}$, when the crystal is moved from air to a liquid. It turns out from such an analysis that the observed changes in D correspond to increases in temperature of less than 2 °C in both modes. An extrapolation of this prediction to the maximum decrease in frequency induced by an increase in temperature of the bulk solution reveals that the corresponding values would be

(23) Filler, R. L. *Proc. 39th Annu. Symp. On Frequency Control*, 311−316.

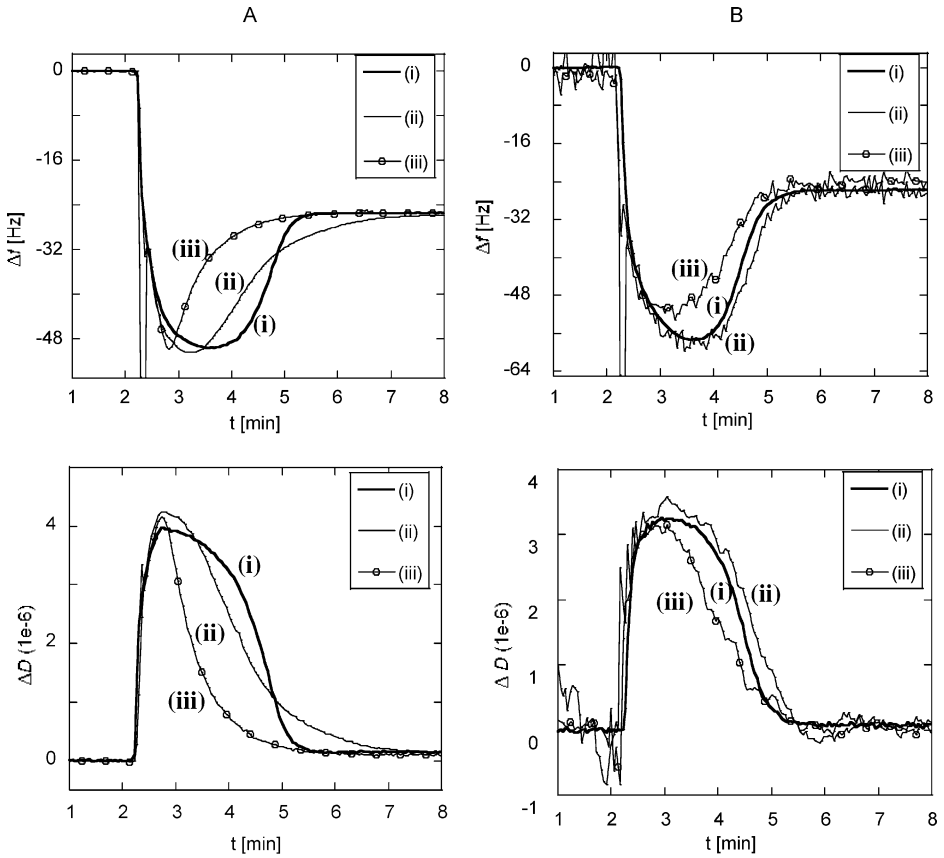

Figure 4. Changes in f ($\Delta f/n$, where n is the overtone number) and D upon exposure of a SiO_2 surface to lipid vesicles at increasing drive amplitudes: (i) 0, (ii) 5, and (iii) 10 V, in mode I (A) and mode II (B). The symbols in (iii) are added as a help for the eye.

+6 Hz in mode I and +10 Hz in mode II. These values are significantly lower than those observed (Figure 3B,D), which means that piezoelectric stiffening of the crystal, and not a temperature increase, is the dominating source of the observed changes in f and D as the applied voltage is varied.[24] Note, however, that the change in frequency at the maximum displacement in the liquid (~36 nm) is larger than the corresponding change in frequency at the same displacement in air (Figure 3A,C), which is attributed to a shift in the peak position as the amplitude of oscillation is increased (see above).

Model System I: Supported Lipid Bilayer Formation. Our first example is lipid−vesicle adsorption on SiO_2, which leads to spontaneous supported lipid bilayer formation. From previous studies, we know in quite some detail the successive steps of the kinetics, see for example, refs 20 and 25−29. We recapitulate the main mechanistic aspects form this prior work, because they are important for our discussion of the amplitude-dependent results that we present below. First, intact vesicles adsorb up to a coverage of ~33% (for the type of lipid used in the present experiments and at ambient temperature), after which they start to rupture and fuse into a planar bilayer. Rupture and fusion (to a bilayer) of adsorbed vesicles occur due to the combined effect of surface interaction, which deforms the vesicles, and vesicle−vesicle interaction, which leads to further deformation. The adsorbed intact vesicles and coupled water (which is the state on the surface preceding bilayer formation) give rise to high dissipation, while the planar bilayer, which forms later on, is much more rigid with almost no dissipation. Additional information has been derived from the T-dependence of this process,[20] which shows that increasing temperature reduces the critical coverage of vesicles, where they start to rupture and fuse to a bilayer. Furthermore, AFM results show that the adsorbed intact vesicles, in the state prior to rupture and fusion, are very fragile and easily induced to rupture by the AFM tip. One additional piece of information, important for the discussion below, is that adsorbed vesicles do not diffuse spontaneously on the surface, but are very close to doing so, since an AFM tip can easily move the vesicles laterally. One might, based on these results, expect an influence of the oscillation amplitude on intact vesicles in the adsorbed state, which was an underlying reason for this choice of model system.

Figure 4 shows changes in f and D upon exposure of a SiO_2 surface to a lipid vesicle suspension at increasing driving voltages (0, 5, and 10 V) obtained in mode I (A) and mode II (B). (The minimum obtainable driving voltage was 50 mV, but is referred to as "0 V".) Inspecting first the data obtained at 0 V, it is clear that the qualitative response is essentially identical in both modes and is interpreted as previously reported for QCM-D analysis of

(24) Bottom, V. E. *Introduction to quartz crystal unit design*; Van Nostrand Reinhold Co.: New York, 1982.
(25) Keller, C. A.; Kasemo, B. *Biophys. J.* **1998**, *75*, 1397−1402.
(26) Keller, C. A.; Glasmastar, K.; Zhdanov, V. P.; Kasemo, B. *Phys. Rev. Lett.* **2000**, *84*, 5443−5446.
(27) Zhdanov, V. P.; Keller, C. A.; Glasmastar, K.; Kasemo, B. *J. Chem. Phys.* **2000**, *112*, 900−909.
(28) Reimhult, E.; Larsson, C.; Kasemo, B.; Höök, F. *Anal. Chem.* **2004**, *76*, 7211−7220.
(29) Richter, R.; Mukhopadhyay, A.; Brisson, A. *Biophys. J.* **2003**, *85*, 3035−3047.

supported lipid bilayer formation.[25] In brief, the initial changes in f and D reflect lipid vesicle adsorption, which continues until a critical surface coverage is reached. At this point, adsorbed vesicles rupture and fuse and the bilayer formation process is initiated. This is reflected in a rapid increase in f and decrease in D, eventually saturating at a change in f of ~ -26 Hz, and a negligible change in D. The slight difference observed between the two modes is attributed to statistical variation and the fact that changes in f and D vary at different harmonics for viscoelastic films.[2,14] As the voltage is increased, the temporal variation in f and D at 5 V in mode I (5 MHz) (where the oscillation amplitude is large) is significantly different from that at 0 V. In strong contrast, the response at 5 V in mode II (35 MHz) remains identical to that at 0 V. At 10 V in mode II, the response resembles that at 5 V in mode I (see Figure 4A). Note, however, that the f and D values at saturation remain unaffected by the increase in oscillation amplitude in all cases; i.e., a supported lipid bilayer is always formed, independent of oscillation amplitude.

Analyzing these data, we need to address several components in the bilayer formation process, which might be affected by the amplitude of oscillation of the surface. The first two are (i) the possibility of a temperature rise of the surface and (ii) the potential influence of the oscillation on the mass-transfer and sticking processes. As argued below, we believe that these two factors can be ruled out as the prime sources of amplitude influence on the whole process. The next three factors that we address are related to (iii) the influence of the amplitude on the binding and shape of vesicles on the surface, (iv) the way the amplitude might influence the mobility of vesicles on the surface, and (v) the potential direct influence of the amplitude on the rupture of adsorbed vesicles.

(i) Temperature Rise due to Dissipated Power in the Sensor. Since the bilayer formation kinetics at higher amplitudes resembles that previously observed in our group at high temperatures,[30] one might suspect that a temperature increase, due to the increasing dissipated power as the driving amplitude is increased, is responsible for the observed effect. Indeed, heating is expected to be larger in mode I than in mode II, which would also be in agreement with the observations (see Figure 4). However, comparing the present data with the previously measured T-dependence, we note that a change in kinetics of the magnitude observed here would require an increase in temperature of $\sim$10 °C.[30] Since the temperature increase in the present case is less than $\sim$2 °C in both modes (see above), a temperature increase is regarded as unlikely to be the dominating factor influencing the kinetics of bilayer formation, when the amplitude is increased. Furthermore, if a temperature increase alone was responsible for the observed effects, the depth of the minimum in f should be larger as the voltage (power) decreases.[30]

(ii) Mass Transport of Vesicles and Sticking Process. First, we assume that the motion in the liquid, induced by the oscillating surface, does not increase the deposition rate of lipid vesicles. This is a reasonable assumption, since we know from previous studies that the adsorption rate of vesicles is mass transport limited.[26] Therefore, possible details of the sticking process of vesicles that might be affected by the increased shear oscillation are not important, unless the effect is very large (one or more orders of magnitude), which is unlikely. The next question is then whether the oscillation might affect the mass transport. This is not impossible, but the fact that the initial rate of change in f versus time is nearly constant as the amplitude of oscillation is increased, suggests that this effect is small, and it is thus reasonable to assume the same mass transport limited binding at all amplitudes. This means that the surface, at all amplitudes, is covered by the same number of vesicles at a given point in time, during the initial phase of adsorption (prior to the peaks in $-\Delta f$ and ΔD).

Hence, we are lead to conclude that the differences observed in Δf and ΔD, in the exposure range prior to the peaks, at the different driving amplitudes, reflect an oscillation-induced change in the structure of the adsorbed vesicles, rather in their number, and that a temperature increase due to the driving power is a minor effect. Next we consider (iii)−(v) above, i.e. the possible influence of the oscillation amplitude on (iii) the adhesion and shape, (iv) on the lateral mobility, or (v) on the rupture/fusion conditions of vesicles. The first two effects are likely to delay (in terms of time/coverage) the onset of rupture /fusion, while the last one will have the opposite effect.

(iii) Influence of Amplitude on the Adhesion and Shape of Vesicles: There are significant differences in the f curves for 0 V and the higher voltages, as the coverage approaches the critical coverage for rupture (Figure 4). Since the adsorbed lipid mass is the same at each point in time independent of amplitude, as argued above, and since changes in f also include water mass hydrodynamically coupled to adsorbed vesicles, this indicates that different amounts of water are entrapped in the film at different amplitudes. One possible explanation is a reduction in surface-induced deformation of the adsorbed vesicles at higher amplitudes; higher amplitudes may partly detach the vesicles from the surface so that they adopt a more spherical shape, which will entrap more water both within and between adjacent vesicles on the surface. This interpretation is further supported by the fact that the ratio between $\Delta D(t)$ and $\Delta f(t)$, which is known to reflect a coverage-independent measure of adsorption-induced structural changes,[26] is clearly different in the three cases analyzed in mode I. There is however, a problem with this reasoning, when we compare with the experimental data: Based on combined experimental and simulation work in our group,[27] less deformed and more spherical vesicles are expected to increase the number of adsorbed vesicles required for rupture to be initiated. Based on this analysis, the peaks in Δf and ΔD would then be expected to be delayed in time/requiring higher coverage, which is in contradiction to our observations (the higher the amplitude, the earlier appear the peaks). This does not rule out this detachment mechanism, however, since it may be operative simultaneously with the other mechanisms iv and especially v.

(iv) Amplitude-Enhanced Mobility of Vesicles. From AFM studies, we know that the vesicles are on these time scales immobile after adsorption. However, they can be moved laterally by the AFM tip; i.e., they are on the verge of being able to diffuse thermally. It is thus not unlikely that the shear oscillation may induce lateral mobility on the surface. If that is the case, it will have a significant, maybe profound, influence on the kinetics. Laterally mobile vesicles will enhance the relaxation of lateral stresses in the layer of vesicles, caused by the combined action of vesicle−surface and vesicle−vesicle interaction. This will in turn

(30) Reimhult, E.; Höök, F.; Kasemo, B. *Phys. Rev. E* **2002**, *66*.

delay the onset of rupture and fusion (which is at variance with the experimental observation of how the minimum in Δf depends on amplitude), but which (possibly together with iii) may explain why the 5-V curve in mode II is so shallow beyond the minimum. Note that roughness is expected to play a critical role for this effect, an issue that was not addressed in the present work, but controlling roughness might help in elucidate this factor.

(v) Amplitude-Induced Rupture. This is the only effect that we can identify to explain that the minimum in Δf appears at shorter times/lower coverage, as the amplitude is increased. Indeed, it is actually a quite likely mechanism. Based on our established model, an increase in coverage leads to an increase in close packing of vesicles and hence an increase in local stress. If there is an external oscillating force, above some threshold, it is likely that this force induces rupture at a lower close packing then at low oscillation amplitudes.

Summarizing our arguments under (i)−(v), we find that (i) and (ii) are not likely primary mechanisms, that (iii)−(v) are all likely to be operative, and that (v) seems to be the main mechanism responsible for the motion of extremum points of the $\Delta f(t)$ and $\Delta D(t)$ curves to lower coverage, while (iii) and (iv) are likely to influence the detailed shapes of the curves. It is not our intention to perform a much deeper analysis along these lines, which would require more detailed experimental data. The important point is that this model system illustrates that the oscillation amplitude can be used to influence the kinetics of adsorption of adsorbed biological entities. In relation to (v) above, there is, however, one aspect that we judge interesting to articulate a little more, namely, how the shear acoustic wave from the sensor surface transplants into the adlayer of vesicles. In doing so, we remind that the oscillation of the surface is coupled to the solution via a layer of *nonrigid* vesicles. Since there is an almost perfect density match between the vesicles and the surrounding liquid, adsorbed vesicles are expected to follow the motion of the crystal without experiencing a significant force of inertia. However, the viscoelastic nature of the nonrigid film will result in exponentially decaying amplitude profiles not only in the bulk liquid but also through the adsorbed vesicles. This will, in turn, induce a shear stress in the vesicles:

$$\tau = G(\Delta x/y) \tag{6}$$

where G is the shear modulus of the vesicles, Δx is the maximum shear displacement, and y is the vesicle film thickness. Although the probed film is composed of discrete macromolecular assemblies, the fact that water is efficiently coupled both within and between adsorbed vesicles[28] makes it reasonable to represent, to a first approximation, the film with a homogeneous thickness (of 12.5 nm[28]), density (of 1.06 kg/m^3 [28]), viscosity (of $> 5 \times 10^{-3}$ kg/ms[28]), and shear modulus (of $\sim 5 \times 10^5$ Pa[28]). By solving the shear-wave propagation through a homogeneous viscoelastic film in an aqueous medium,[21] Δx^{max} was estimated to be 0.15 and 0.08 nm in mode I and mode II, respectively. This, in turn, is equivalent to a maximum shear stress of ~6 and 3.2 kPa in mode I and mode II, respectively. Assuming that each vesicle occupies a circular area with a radius of 35 nm,[28] the shear force experienced by individual vesicles will be ~25 and 14 pN in mode I and mode II, respectively. Although these estimates must be considered rough

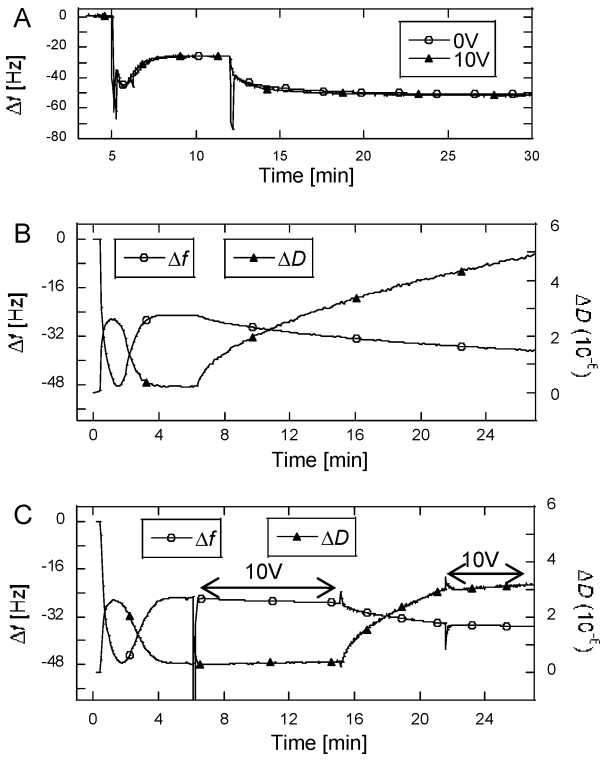

Figure 5. (A) Changes in f upon the formation of a biotin-containing supported lipid bilayer, followed by the addition of streptavidin at high (10 V) and low (0 V) driving voltages in mode I. (B) Changes in f and D versus time upon the addition of NeutrAvidin-coated spheres (o.d. ~200 nm) to a biotin-containing supported lipid bilayer (cf. Figure 4) at low (0 V) and (C) high (10 V) at driving voltage in mode I. Also shown in (C) are changes in f and D versus time ($t \sim 15$ min) upon decreasing the drive voltage from 10 to 0 V, followed by an increase to 10 V at $t \sim 22$ min. The minimum obtainable driving voltage was 50 mV, but is referred to as "0 V".

approximations, it is interesting to note that the higher value is one-quarter to a half of the minimum force that has been reported to induce rupture of vesicles on SiO_2 using contact-mode AFM imaging. In fact, spontaneous rupture of vesicles on an individual basis, as observed using AFM, was not observed in the present study, but rather an influence of the dynamics of the bilayer formation process, which appears likely in this force regime. An alternative picture emerges if the adsorbed vesicles are instead considered as discrete objects through which the amplitude of oscillation decays with a longer decay length than that of the liquid surrounding the adsorbed vesicles. In such a case, the velocity difference between the vesicles and the surrounding liquid will induce a torque[31] that will deform and destabilize the lipid membrane and hence contribute to an earlier onset of the rupture process. Irrespective of which model that best represents the current situation, it is clear that a shear stress in the film is likely and that this mechanism will promote the rupture process.

Protein and Colloidal Particle Binding. To investigate the influence of elevated amplitudes on molecular recognition reactions, specific binding of streptavidin (0.15 μM, M_w ~65 kDa) to a biotin-modified supported bilayer was investigated in mode I at nominal driving voltages of 0 and 10 V (Figure 5). First, a biotin-containing supported bilayer was formed as described above. The

(31) Chang, K.-C.; Hammer, D. A. *Langmuir* **1996**, *12*, 2271−2282.

biotin molecules in the bilayer create binding sites for the protein streptavidin, which otherwise do not bind to the bilayer. The biotin "doped" bilayer was then exposed to a streptavidin solution at 0 and 10 V_{pp}, and no detectable difference was observed between the two cases. The same observation was also made in mode II. Another similar case was tested. Instead of biotin in a bilayer, we adsorbed, on a gold surface, albumin (BSA) molecules with biotin groups attached, and then this surface was exposed to streptavidin. The same result was obtained as with the biotin doped bilayer, i.e., no amplitude-induced changes. It can thus be concluded from these data that the force induced at oscillation amplitude of 36 nm at 5 MHz is not sufficient to influence the streptavidin−biotin interaction either in a laterally mobile or in an immobile film.

To further increase the maximum attainable oscillation-induced force on the molecular bond, streptavidin was replaced by 200-nm polystyrene spheres (~11 pM) that were coated with NeutrAvidin (a streptavidin analogue). Upon exposure of a biotin-doped supported bilayer to such spheres, the amount bound (after ~10 min) at a nominal driving amplitude of 10 V was reduced to <20% of that recorded at low driving amplitude (Figure 5). However, upon increasing the driving amplitude *after* adsorption of a significant amount of spheres at low driving amplitude, no desorption was observed. (The same effect was observed when the bilayer was replaced by a PLL−PEG layer with biotin or biotin-modified BSA, which renders adsorption of immobile colloidal particles, while the lipids in the bilayer are laterally mobile.) These results show that the applied amplitude is indeed sufficient to inhibit binding to some degree, but not sufficient to induce rupture of already established bonds of the strength typical for biotin−streptavidin. (Sufficiently weak bonds may—or are even likely—to be subject to rupture.) In analogy with the case of adsorbed lipid vesicles, the almost perfect density match between polystyrene spheres (1.05 g/cm^3) and water (1 g/cm^3) and their small size makes the force of inertia negligible. However, in contrast to the vesicles, polystyrene beads can be considered as perfectly rigid under these conditions, which implies that particle deformation should not occur. For the same reason, the amplitude of oscillation will remain constant through attached particles and the velocity difference between an attached particle and the liquid surrounding the particles is expected to induce a notable torque. Since a substantial amount of water is coupled as a more or less rigid mass to the particles, through which the oscillation decay is hard to estimate, it is difficult to estimate this torque quantitatively. Still, it is interesting to note that binding can be inhibited, but not broken, which means that the induced force approaches the range required to influence the biotin−streptavidin bond, which from force spectroscopy data has been estimated to be between ~5 and ~200 pN depending on load rate.[32] The fact that established bonds cannot be broken in this case, while their formation can be inhibited to some degree, is not too surprising. Once the bond is formed, the force is obviously not enough to break it. However, for bond formation, one also has to consider the kinetics—or rather dynamics—of binding. The oscillatory motion can very well affect the potential energy surface and the many low-lying energy states of proteins that are known to exist, making the entrance channel to bond formation more restricted. Both theory[33] and experiments[32] suggest that at least one shallow intermediate state must be passed in order to reach the deepest energy minimum. Although an explicit value of the strength of the shallow minimum does not, to the best of our knowledge, exist, the force required to prevent the establishment of this state is expected to be significantly lower than that required to rupture the equilibrated bond.

An alternative explanation of the observed results is that, upon approach, binding will not occur if the establishment of a single NeutrAvidin−biotin bond is inhibited. Once bound, however, the lateral mobility of biotin moieties in the supported bilayer might lead to the establishment of multiple bonds, which will require significantly higher forces break. However, the NeutrAvidin coverage (~70 molecules per sphere) makes the involvement of more than one NeutrAvidin molecule highly unlikely, and the fact that the same pattern was observed when (i) the biotin−lipid fraction was dramatically reduced and (ii) biotin was immobile on the surface makes this explanation less likely.

CONCLUDING REMARKS

By extending the QCM-D technique to operate in dual-frequency mode, we were able to conduct combined f and D measurements, while simultaneously influencing various surface-binding reactions via elevated oscillation amplitudes. The typical driving amplitude (1 V) used in traditional decay-based measurements had no influence on any of the systems investigated: i.e., spontaneous supported lipid bilayer formation on SiO_2, streptavidin binding to a biotin-modified substrate and binding of NeutrAvidin-coated polystyrene spheres (o.d. ~200 nm). Via an increase in the shear stress experienced by adsorbed vesicles, the kinetics of supported lipid bilayer formation on SiO_2 is influenced at oscillation amplitudes larger than ~11 and ~0.75 nm at 5 and 35 MHz, respectively, while no influence is observed on streptavidin binding. Although the latter finding contradicts one of the previous results obtained for protein adsorption,[34] we consider our data to be reliable and applicable to most macromolecular assemblies of sizes comparable to typical globular proteins (10 kDa < M_w < 200 kDa).

When the mass of the interacting components was increased by 4 orders of magnitude, we were able to prevent binding, but no signs of desorption were observed. This is in contrast to the recent work in Klenerman's group,[16−18] demonstrating solid proofs of bond rupture of specifically attached colloidal and virus particles with a size and density comparable to that of the colloidal particles used in the present study. These somewhat conflicting results are attributed to the facts that (i) they used plano-convex crystals, which increases the maximum oscillation amplitude, (ii) the virus particles were of irregular shape, which may increase the torque experienced, and (iii) the antibody−antigen binding was of weaker strength in the case of the virus particles. Future work will focus on experimental conditions enabling both binding and rupture events to be monitored in real time via combined f and D measurements, to map out the interaction energy landscape in these frequency intervals.

(32) Merkel, R.; Nassoy, P.; Leung, A.; Ritchie, K.; Evans, E. *Nature* **1999**, *397*, 50−53.
(33) Grubmüller, H.; Heymann, B.; Tavan, P. *Science* **1996**, *271*, 997−999.
(34) Wang, A. W.; Kiwan, R.; White, R. M.; Ceriani, R. L. *Sens. Actuators B* **1998**, *49*, 13−21.

ACKNOWLEDGMENT

We thank Dr. M. Zäch, Dr. J. Benkoski, C. Larsson, and I. Pfeiffer, all at the Chalmers University of Technology, Gothenburg, for valuable discussions. We also like thank our collaborators at the Laboratory for Surface Science and Technology, ETH-Zürich for generously providing the biotin−PLL−PEG. Financial support from the Swedish Research Council for Engineering Sciences, Contract 2000-175, is gratefully acknowledged.

Received for review January 20, 2005. Accepted May 10, 2005.

AC050116J